Ice-assisted electron beam lithography of graphene

Jules A Gardener[1] and Jene A Golovchenko[1,2]

[1]Department of Physics, Harvard University, Cambridge, Massachusetts 02138, USA

[2]School of Engineering and Applied Sciences, Harvard University, Cambridge, Massachusetts 02138, USA

E-mail: golovchenko@physics.harvard.edu

Abstract. We demonstrate that a low energy focused electron beam can locally pattern graphene coated with a thin ice layer. The irradiated ice plays a crucial role in the process by providing activated species that locally remove graphene from a silicon dioxide substrate. After patterning the graphene, the ice resist is easily removed by sublimation to leave behind a clean surface with no further processing. More generally, our findings demonstrate that ice-assisted e-beam lithography can be used to pattern very thin materials deposited on substrate surfaces. The procedure is performed *in situ* in a modified scanning electron microscope. Desirable structures such as nanoribbons are created using the method. Defects in graphene from electrons backscattered from the bulk substrate are identified. They extend several microns from the e-beam writing location. We demonstrate that these defects can be greatly reduced and localised by using thinner substrates and/or gentle thermal annealing.

PACS: 07; 61; 68; 79

1. Introduction

With recent interest in nanoscale structures in atomically thin materials, it has become highly desirable to be able to selectively pattern device structures in these materials on nanometer length scales. In graphene, for example, this capability enables the tuning of its photonic [1] or electronic [2, 3] properties. Several lithographic approaches have been developed for this purpose. Typically, polymer resists are deposited onto graphene samples and selected regions are exposed to electron or light beams and developed [1-6]. The exposed graphene is either plasma etched directly [1-4], or a protective metal mask is created by lift-off prior to etching [5, 6]. These approaches require a large number of steps and the use of polymer resists and/or masks, which can leave a detrimental residue on graphene [7].

Other methods have been developed which use an SEM beam to directly remove graphene [8] and other materials [9]. In these approaches, the electron beam generates reactive species from a surrounding vapour which chemically etch the surface. It is also known that direct exposure of graphene to an electron beam creates defects [10, 11]. This damage has been characterized by a so-called amorphization trajectory, wherein graphene converts to nanocrystalline graphite and then to sp^2 amorphous carbon with increasing electron dose [12].

Here we show that graphene covered by a thin ice layer can be etched by a patterning electron beam. An overview of the procedure is given schematically in Figure 1. Briefly, a thin ice layer is grown on the graphene surface (Figure 1(a)) and selected regions are exposed to an electron beam (Figure 1(b)). The remaining ice is then removed, leaving a pattern in the graphene layer that has been etched away in the exposed regions (Figure 1(c)). This simple procedure is performed *in situ* in an electron microscope and doesn't require the use of polymer resists or metals. Instead, the ice layer protects the unexposed graphene surface from e-beam deposited contaminants and is easily removed to leave behind a clean surface.

2. Experimental details

Both chemical vapour deposited (CVD) graphene and cleaved graphene flakes were used in this study. Single layer CVD graphene was grown on a copper foil from methane gas [13]. The CVD graphene was coated with a thin methyl methacrylate (MMA) support layer for $FeCl_3$ etching of the Cu foil and subsequent transfer to a 300nm SiO_2 on Si substrate [14]. The MMA layer was then removed by immersion in acetone and isopropanol. The cleaved graphene flakes were obtained by mechanical exfoliation of graphite and deposited onto the SiO_2(300nm)/Si substrate [15]. All samples were then cleaned by heating in 0.4L/min H_2 gas flow at 300C. The graphene quality and thickness were subsequently verified using scanning confocal Raman spectroscopy (WiTec, 532nm excitation, 1.1mW).

These samples were cooled to ~-165C under vacuum ($5x10^{-7}$Torr) in a custom designed e-beam writing, field emission, scanning electron microscope (SEM) [16]. A 100-200nm thick amorphous ice layer was vapour deposited onto the cold surface. Surface regions 2µm x 10µm were then exposed to a 3-15kV, 2nA electron beam and e-beam doses of 0.4-2.0C/cm^2 were used to explore the graphene/ice etching process. After e-beam exposure, the samples were briefly imaged with the electron beam at low doses (10^{-6}-10^{-8}C/cm^2) and then the remaining ice was removed by sublimation in the microscope at -100C. The samples were then warmed to room temperature and removed from the vacuum for further study.

Post-processing sample evaluation was performed with a Nikon Eclipse ME600L optical microscope (bright field white light illumination), the aforementioned scanning Raman spectrometer and an Asylum Research atomic force microscope (AFM) in tapping mode.

3. Results and discussion

3.1 Characterization of e-beam etched graphene

Figure 2(a) shows an optical microscope image of single layer CVD graphene that was exposed to a dose of 1.8C/cm^2 15kV electrons in a rectangular region through 130nm ice. The exposed graphene free region appears as a bright rectangle. The contrast variation between the remaining graphene layer and the brighter exposed region is identical to that observed across a cleaved graphene edge.

Graphene Raman spectra obtained ~3μm away from the exposed region (Figure 2(b), red) show peaks at ~1586cm^{-1} and ~2679cm^{-1}, the so-called G and 2D peaks, which arise from sp^2 C-C bond stretching and C ring breathing modes respectively [12]. No such peaks are observed in the exposed rectangle (Figure 2(b), blue), confirming the absence of graphene in this region. Analogous etching results are obtained for both single and bilayer graphene using 3-15kV e-beams.

3.2 The role of ice

A key difference between the procedure presented here and conventional e-beam lithography is the use of ice as a resist. E-beam exposure of graphene in the absence of ice significantly modifies the graphene from its original form (Figure 2(c)). Specifically, the Raman spectrum is characteristic of amorphous sp^2 carbon, wherein the so-called D peak (which arises from the presence of defects) appears at ~1347cm^{-1}, while the 2D peak intensity is greatly reduced [12]. We therefore conclude that exposure through ice fully removes graphene.

The electron energies used in the SEM are well below the 86keV required for direct recoil removal of carbon atoms from graphene [17]. Instead, the graphene removal must be a chemical effect resulting from the exposure of graphene to H [18], O [19] and other excited dissociation fragments [20,21] created as the e-beam interacts with the ice. We propose that carbon atoms are removed by the reaction of dangling carbon bonds initially created by the e-beam and subsequent interaction with the electron stimulated H_2O dissociation products, forming small carbon containing volatile molecules (e.g. CO, CO_2 …) that desorb

from the surface. It is interesting to note that on an ice covered clean silicon surface the reaction products are not volatile and a thin SiO_2 layer is grown instead [22].

An important advantage of the use of ice is that it is readily removed by sublimation and leaves much less residue than conventional e-beam resists [23]. Figure 3(a) shows an AFM image of CVD graphene after e-beam irradiation and ice removal (this is the same sample as shown in Figure 2(a)-(b)). The linescan below the AFM image shows that the exposed region is ~3nm lower than the surrounding region. This is due to graphene removal and e-beam induced volume reduction of the amorphous SiO_2 substrate [24]. The remaining graphene region has a root-mean-square surface roughness of 0.48-0.52nm. Thin wrinkles and small patches of multilayer graphene are observed in the unexposed region, as is typical for CVD graphene [13]. In addition, the surface is slightly raised in the vicinity of the etched region, presumably due to local changes in the graphene morphology (as will be discussed shortly) or e-beam induced modification of the underlying substrate [24]. Otherwise, the surface is featureless, confirming that the ice layer has not introduced significant surface contamination.

3.3 Fabrication of graphene ribbons

It has already been demonstrated that structures as small as 10nm can be fabricated with ice lithography [16, 22]. Therefore, it is relatively straightforward to create more complex and much smaller patterns in graphene by this procedure. For example, Figure 3(b) shows an AFM image of graphene nanoribbons created from a cleaved single layer graphene flake by a 5kV e-beam through a 130nm ice layer. The nanoribbons are seen as bright lines on that are ~2nm higher than the surrounding SiO_2/Si substrate. The ribbons shown in Figure 3(b) are 50nm and 59nm wide and 3μm in length, with the latter dimension limited by the dimensions of the graphene flake.

3.4 Graphene damage and reduction

Ice lithography requires ~10^3 larger electron doses than conventional e-beam lithography [22, 23]. One may anticipate graphene damage induced by backscattered electrons returning to the surface from the bulk many microns from where the incident e-beam enters the surface. We constructed spatial Raman maps of this damage near an etched region. These Raman images have a resolution of ~1μm, limited by the incident laser spot size. Figures 4(a-b) show maps of the integrated D and G peak intensities (which we denote I(D) and I(G) respectively where $1261<I(D)<1453cm^{-1}$, $1536<I(G)<1612cm^{-1}$) for the sample region shown in Figure 2(a)-(b). The exposed rectangle appears black in both maps, consistent with Figure 2(b), while a bright halo extends out to ~2μm in the D peak map, signifying significant damage induced near the e-beam exposure. Full Raman spectra taken in (i) the irradiated region, (ii) the box edge, (iii) 1μm from the edge and (iv) 2μm from the edge are shown in Figure 4(c). The edge Raman spectra (Figure 4(c)(ii)) has a lineshape characteristic of amorphous carbon [12] whereas the graphene becomes less damaged with increasing distance from the graphene edge (Figure 4(c)(iii)-(iv)). Typical integrated I(D)/I(G) ratios are plotted versus distance from the etched edges (Figure 4(e), red traces) and peak at ~1μm. At smaller distances these ratios fall due to formation of partly sp^2 amorphous carbon [12]. Annealing in 0.6L/min Ar at 300C for 1 hour reduces I(D)/I(G) and ideal graphene signals are obtained for all but the amorphous C region [25] near the graphene edge, as shown in Figure 4(d).

To confirm our interpretation of the spatial extent of the graphene damage, we have simulated 15kV electron trajectories (CASINO software [26]) passing through a 130nm ice layer and a SiO_2(300nm)/Si substrate. The results of these simulations for 1000 primary electron trajectories are shown in Figure 5(a). The e-beam spreads by ~40nm due to multiple scattering events during its passage through the ice. But scattering in the substrate returns a component of the beam to the surface and spreads it out laterally by ~1.9μm from the position of the incident beam, a distance consistent with the extent of the damage in Figure 4(a). This suggests that using a substrate much thinner than the electron range (~2.4μm at 15kV) should result in greatly reduced graphene damage. To test this, we prepared graphene samples on 40nm

thick SiO_2 windows (Ted Pella) and e-beam etched these under the same conditions as the sample in Figure 4(a,b). The Raman maps (Figure 6(a,b)) show reduced damage spread. Full Raman spectra taken at the edge of the exposed region (Figure 6(c)(ii)) show that the graphene in this region has been less severely modified by the electron beam, compared with the case on bulk SiO_2(300nm)/Si (Figure 4(c)(ii)). All Raman spectra show that some damage is present, presumably from post-write imaging (which was necessary to locate the exposed region for Raman analysis). However, I(D)/I(G) ratios within the innermost 2 μm on the thin membrane substrate (Figure 6(e), red) are generally much lower than those on SiO_2(300nm)/Si (Figure 4(e)), confirming that reducing the substrate thickness reduces the degree of damage. The spatial resolution of the Raman spectrometer does not allow us to quantitatively determine a lower limit to the spatial extent of the damage. However, simulations suggest that 95% of electron trajectories are contained within 40nm from the incident beam location for 130nm ice on 40nm SiO_2 (Figure 5(b)), with the majority of scattering events occurring in the ice layer. Figure 6(d) shows that defects arising from exposure or post-write imaging are greatly reduced by annealing, with a maximum integrated I(D)/I(G) ratio of ~0.9 at the edge. We measured I(D)/I(G) at a cleaved graphene flake edge (not subjected to e-beam exposure) and obtain ~0.4. This can be taken as a measure of the intrinsic Raman signal from a pristine graphene edge, while the e-beam cut edges are likely to have a higher atomic-scale roughness than cleaved graphene (and so we expect to measure a higher I(D)/I(G) ratio for our samples). We therefore conclude that the vast majority of beam induced damage on the thin substrate has been annealed out.

4. Conclusion

We have demonstrated that an electron beam can be used to remove graphene when exposed through a thin ice layer. A variety of structures can be fabricated using this approach, which is simple, capable of nanoscale resolution patterning and eliminates surface contamination characteristic of polymer resist

based methods. Reducing the substrate thickness and gentle annealing can limit e-beam induced defects in the vicinity of the etched region by reducing backscattered and secondary electron induced damage from the substrate. The latter finding is also applicable to graphene structures fabricated using conventional e-beam lithography with polymer resists, wherein backscattered electrons and scattering in the polymer resist can also create damaged structures. Future work should clarify the atomic structure of the etched edges and, if needed, examine ways to control it [27-29]. It may be anticipated that the new process demonstrated here may also be used to etch patterns in thin layers other than graphene when appropriate reaction products for etching are released from the condensed layer above it.

Acknowledgments

The authors thank B. Hubbard, Dr. S. Garaj, Dr. A. Han, Dr. C. Russo, Dr. F. Albertorio and Prof. D. Branton for helpful discussions and P. Frisella for technical assistance. Dr. S. Garaj and S. Liu grew the CVD graphene. This work was supported by National Institutes of Health Award R01HG003703 to J. A. Golovchenko and was partly performed at Harvard University's Center for Nanoscale Systems (CNS).

References

[1] Ju L, Geng B, Horng J, Girit C, Martin M, Hao Z, Bechtel H A, Liang X, Zettl A, Shen Y R and Wang F 2011 *Nature Nano.* **6** 630-4

[2] Han M Y, Ozyilmaz B, Zhang Y and Kim P 2007 *Phys. Rev. Lett.* **98** 206805

[3] Chen Z, Lin Y-M, Rooks M J and Avouris P 2007 *Physica E* **40** 228-32

[4] Stampfer C, Guttinger J, Molitor F, Graf D, Ihn T and Ensslin K 2008 *Appl. Phys. Lett.* **92** 012102

[5] Wang X and Dai H 2010 *Nature Chem.* **2** 661-5

[6] Lian C, Tahy K, Fang T, Li G, Xing H G and Jena D2010 *Appl. Phys. Lett.* **96** 103109

[7] Fan J, Michalik J M, Casado L, Roddaro S, Ibarra M R and De Teresa J M 2011 *Solid State Commun*. **151** 1574-78

[8] Fox D, O'Neill A, Zhou D, Boese M, Coleman J N and Zhang H Z 2011 *Appl. Phys. Lett.* **98** 243117

[9] Randolph S J, Fowlkes J D and Rack P D 2006 *Crit. Rev. Solid State* **31** 55-89

[10] Teweldebrhan D and Balandin A A 2009 *Appl. Phys. Lett*. **94** 013101

[11] Xu M, Fujita D and Hanagata N 2010 *Nanotechnology* **21** 265705

[12] Ferrari A C 2007 *Solid State Commun.* **143** 47-57

[13] Li X, Cai W, An J, Kim S, Nah J, Yang D, Piner R, Velamakanni A, Jung I, Tutuc E, Banerjee S K, Colombo L and Ruoff R S 2009 *Science* **324** 1312-14

[14] Li X, Zhu Y, Cai W, Borysiak M, Han B, Chen D, Piner R D, Colombo L and Ruoff R S, 2009 *Nano Lett.* **9** 4359-63

[15] Novoselov K S, Geim A K, Morozov S V, Jiang D, Zhang Y, Dubonos S V, Grigorieva I V and Firsov A A, 2004 *Science* **306** 666-9

[16] Han A, Chervinsky J, Branton D and Golovchenko J A, 2011 *Rev. Sci. Instr*. **82** 065110

[17] Smith B W and Luzzi D E 2001 *J. Appl. Phys.* **90** 3509-15

[18] Petrik N G and Kimmel G A 2003 *Phys. Rev. Lett*. **90** 166102

[19] Sieger M T, Simpson W C and Orlando T M 1998 *Nature* **394** 554-556

[20] Stulen R H and Thiel P A 1985 *Surf. Sci.* **157** 99-118

[21] Rowntree P, Parenteau L and Sanche L 1991 *J. Chem. Phys.* **94** 8570-8576

[22] King G M, Schurnann G, Branton D and Golovchenko J A 2005 *Nano Lett*. **5** 1157-60

[23] Han A, Vlassarev D, Wang J, Golovchenko J A and Branton D 2010 *Nano Lett.* **10** 5056-9

[24] Stevens Kalceff M A, Phillips M R and Moon A R 1996 *J. Appl. Phys.* 80 4308-14

[25] Teweldebrhan D and Balandin A A 2009 *Appl. Phys. Lett*. **95** 246102

[26] Drouin D, Couture A R, Joly D, Tastet X, Aimez V and Gauvin R 2007 *Scanning* **29** 92-101

[27] Begliarbekov M, Sasaki K-I, Sul O, Yang E-H and Strauf S 2011 Nano Lett. **11** 4874-4878

[28] Jai X et al., 2009 Science **323** 1701-1705

[29] Nemes-Incze P, Magda G, Kamaras K and Biro L P 2010 Nano Res. **3** 110-116

FIGURES

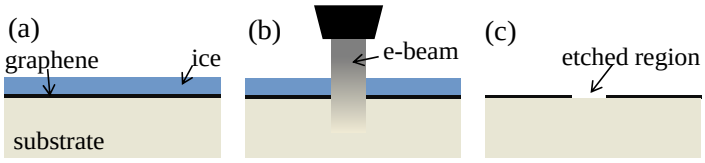

FIGURE 1. (Colour online) Overview of the graphene etching procedure. (a) An amorphous ice layer (blue) is grown on graphene (black) on a substrate (beige). (b) Selected regions are then exposed to an electron beam (grey). (c) The ice is sublimed *in situ*, leaving behind the etched graphene layer.

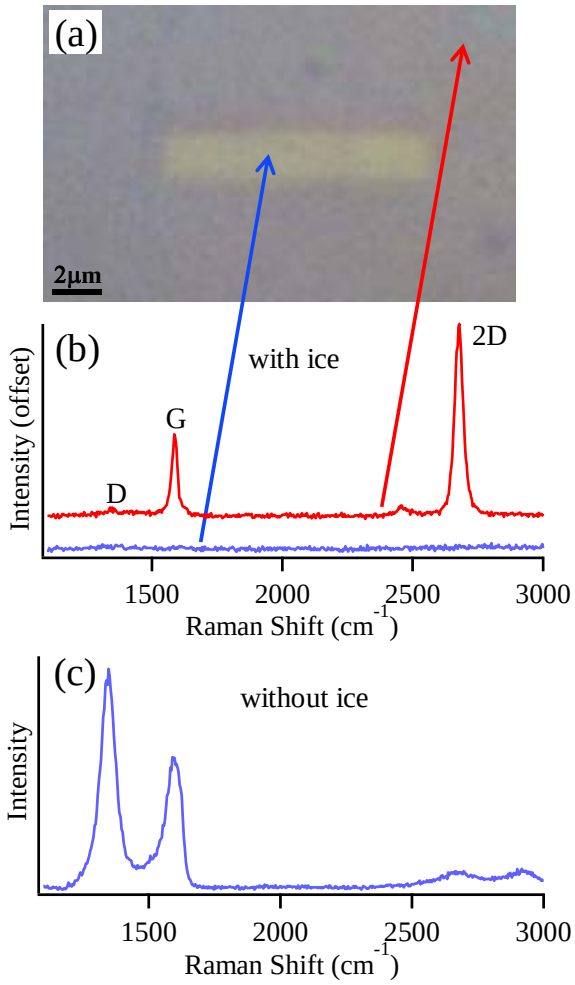

FIGURE 2. (Colour online) Characterization of the exposed graphene regions. (a) Optical microscope image of graphene on SiO_2(300nm)/Si that has been exposed to an e-beam via an ice layer. (b) Raman spectra obtained from the same sample at the locations indicated by arrows (spectra offset for clarity). (c) Raman spectrum of a graphene sample exposed to the same conditions as in (b) except no ice was deposited.

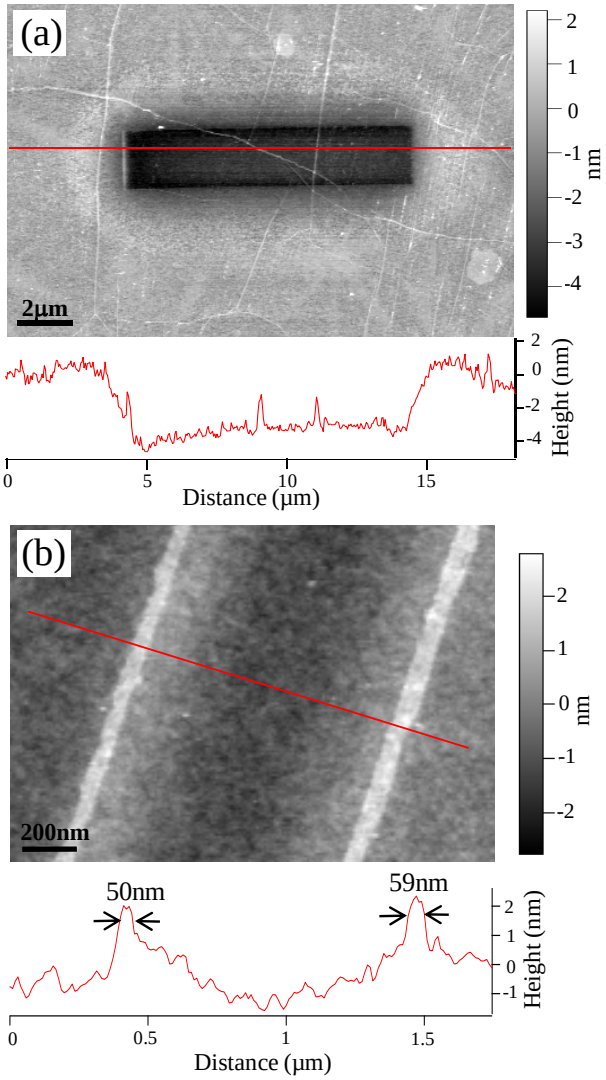

FIGURE 3. (Colour online) Atomic force microscopy images of etched graphene. (a) An AFM image of etched CVD graphene on SiO_2(300nm)/Si. This is the same sample as shown in Figure 2(a)-(b). A linescan taken at the position indicated by a horizontal red line is shown below the AFM image. (b) An AFM image of a graphene nanoribbon array on SiO_2(300nm)/Si (darker background) created from a single layer cleaved graphene flake. A linescan of the section indicated by a red line is shown below the image and the ribbon widths are indicated.

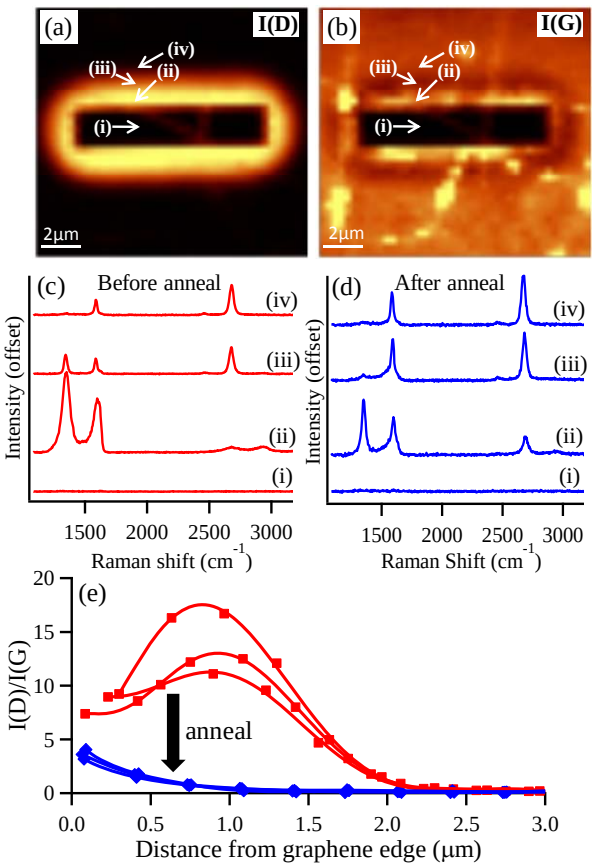

FIGURE 4. (Colour) Raman analysis of graphene damage on a SiO_2(300nm)/Si substrate (this is the same sample as shown in Figure 2(a)-(b)). (a)-(b) Integrated I(D) and I(G) Raman maps respectively of the sample prior to annealing. (c) Raman spectra obtained prior to annealing at various locations, as indicated in (a,b), namely (i) inside the exposed region, (ii) at the graphene edge, (iii) 1μm from the graphene edge and (iv) 2μm from the graphene edge. (d) Analogous Raman spectra to (c) obtained at the same locations of the same sample following a 300C Ar anneal. (e) Typical ratios of the integrated Raman D and G peaks (denoted I(D) and I(G) respectively) as a function of distance from the graphene edges before (red squares) and after (blue diamonds) post-process annealing.

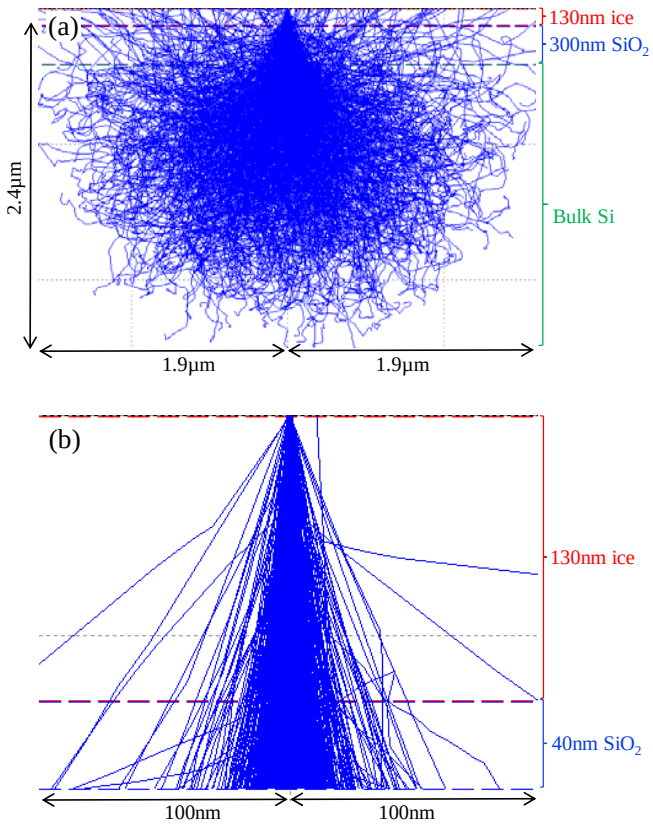

FIGURE 5. (Colour online) Simulations of 15kV primary electron trajectories. (a) Through 130nm ice on a SiO_2(300nm)/Si substrate. (b) Through 130nm ice on a 40nm SiO_2 membrane. These simulations were performed using CASINO software [26] and each show 1000 primary electron trajectories (blue lines).

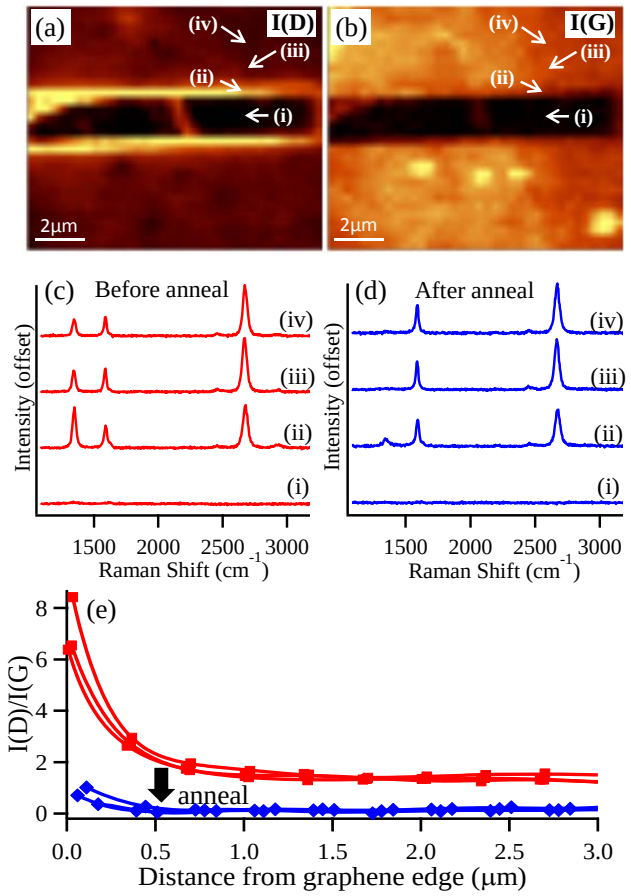

FIGURE 6. (Colour) Raman analysis of graphene damage on a thinner substrate (40nm SiO_2) than shown in Figure 4. (a)-(b) Integrated I(D) and I(G) Raman maps respectively of the sample prior to annealing. (c) Raman spectra obtained prior to annealing (i) inside the exposed region, (ii) at the graphene edge, (iii) 1μm from the graphene edge and (iv) 2μm from the graphene edge. (d) Analogous Raman spectra to (c) following a 300C Ar anneal. (e) Typical ratios of the integrated Raman D and G peaks as a function of distance from the graphene edges before (red squares) and after (blue diamonds) post-process annealing.